CORE
Metadata, citation and similar papers at core.ac.uk
Provided by NASA Technical Reports Server

NASA Technical Memorandum 78637

(NASA-TM-78637) OPERATIONAL EXPERIENCE IN THE LANGLEY EXPANSION TUBE WITH VARIOUS TEST GASES (NASA) 35 p HC A03/MF A01 CSCL 14B

N78-15060

Unclas
G3/09 57783

Operational Experience in the Langley Expansion Tube With Various Test Gases

Charles G. Miller

December 1977

JAN 1978
RECEIVED
NASA STI FACILITY

National Aeronautics and Space Administration
Langley Research Center
Hampton, Virginia 23665

1. Report No.	2. Government Accession No.	3. Recipient's Catalog No.
TM 78637		

4. Title and Subtitle	5. Report Date
Operational Experience in the Langley Expansion Tube With Various Test Gases	December 1977
	6. Performing Organization Code: 6430
7. Author(s): Charles G. Miller	8. Performing Organization Report No.: TM 78637
	10. Work Unit No.: 506-26-23-01
9. Performing Organization Name and Address: NASA Langley Research Center, Hampton, Virginia 23665	11. Contract or Grant No.
	13. Type of Report and Period Covered: Technical Memorandum
12. Sponsoring Agency Name and Address	14. Sponsoring Agency Code: NASA

15. Supplementary Notes

16. Abstract

A resumé of operating experiences with the Langley Expansion Tube is presented. The driver gas was unheated helium at a nominal pressure of 5000 psi (34.5 MN/m^2) and the majority of the data presented herein are for air and carbon dioxide test gases. The primary purpose of these data is to illustrate the effects of various parameters on quasi-steady test flow duration, as well as free stream and postnormal shock flow conditions. The present discussion shows that the Langley Expansion Tube is an operational facility capable of producing good quality, highly repeatable, quasi-steady flow for test times sufficient to establish flow about blunt axisymmetric and two-dimensional models. Due to the capability of testing with arbitrary test gases, a wide range of real-gas, hypersonic-hypervelocity flow conditions may be generated. However, for a given test gas, the range of operating conditions producing useful flow is shown to be rather limited; hence, the facility yields a given flow condition for a given test gas, and variation in flow conditions comes about by using different test gases.

ORIGINAL PAGE IS
OF POOR QUALITY

17. Key Words (Suggested by Author(s))	18. Distribution Statement
Hypersonic; Hypervelocity; Impulse Facility; Real Gas	Unclassified Unlimited

19. Security Classif. (of this report)	20. Security Classif. (of this page)	21. No. of Pages	22. Price*
Unclassified	Unclassified	33	$4.00

* For sale by the National Technical Information Service, Springfield, Virginia 22161

OPERATIONAL EXPERIENCE IN THE LANGLEY EXPANSION TUBE WITH VARIOUS TEST GASES

Charles G. Miller
NASA Langley Research Center
Hampton, Virginia 23665

SUMMARY

A resumé of operating experiences with the Langley Expansion Tube is presented. The driver gas was unheated helium at a nominal pressure of 5000 psi (34.5 MN/m^2) and the majority of the data presented herein are for air and carbon dioxide test gases. The primary purpose of these data is to illustrate the effects of various parameters on quasi-steady test flow duration, as well as free stream and postnormal shock flow conditions. The present discussion shows that the Langley Expansion Tube is an operational facility capable of producing good quality, highly repeatable, quasi-steady flow for test times sufficient to establish flow about blunt axisymmetric and two-dimensional models. Due to the capability of testing with arbitrary test gases, a wide range of real-gas, hypersonic-hypervelocity flow conditions may be generated. However, for a given test gas, the range of operating conditions producing useful flow is shown to be rather limited; hence, the facility yields a given flow condition for a given test gas, and variation in flow conditions comes about by using different test gases.

SYMBOLS

M	Mach number
N_{Re}	Unit Reynolds number
p	Static pressure
p_t	Pitot pressure
$\dot{q}$	Convective heating rate
t	Time after arrival of incident shock into test gas or acceleration gas
T	Temperature
U	Velocity
U_s	Incident shock velocity
W	Secondary diaphragm thickness
γ_E	Isentropic exponent
ϵ	Ratio of density immediately behind standing normal shock to free-stream density
τ	Time interval between arrival of incident shock into acceleration gas and acceleration gas-test gas interface
ψ	Time interval between arrival of acceleration gas-test gas interface and tail of expansion fan
Ω	Measured time interval over which the test gas is quasi-steady

Subscripts

a	Applied
c	Tube center line
ca	Calculated
e	Acceleration section exit
f	Flat-plate surface
s	Static conditions immediately behind a normal standing shock

ORIGINAL PAGE IS
OF POOR QUALITY

sp	Stagnation conditions behind a normal standing shock
w	Acceleration section tube
1	State of quiescent test gas in front of incident shock in intermediate section
2	Test gas conditions behind incident shock in intermediate section
10	State of quiescent acceleration gas in front of incident shock in acceleration section
∞	Free-stream conditions

INTRODUCTION

The level of heating and the aerodynamic performance of vehicles entering Earth or planetary atmospheres vitally affect mission success. Total duplication of the high-velocity entry conditions, particularly for the outer planets, is beyond the capability of existing ground-based facilities and thus computer calculations are relied on heavily in mission design. However, experimental facilities make an important and necessary contribution toward prediction of the entry environment because the computer predictions are generally dependent on empirical input data and are verified by tests performed in various types of facilities, each of which simulates or duplicates certain aspects of the problem. One such facility is the expansion tube. The Langley Expansion Tube is an operational facility[1-3] which is used for hypersonic-hypervelocity aerothermodynamic studies on models representative of candidate entry probes with gases representative of proposed planetary atmospheres.[3-5] Although expansion tube flow characteristics with various test gases have been reported[2,3] for specific test conditions, the evolutionary process leading to the obtainment of the most satisfactory flow conditions has not.

The initial theoretical analyses of the expansion tube,[6] which neglected viscous effects, finite diaphragm opening times, and chemical relaxation rates, suggested that the facility would be extremely

flexible in its operation mode. These idealized performance predictions indicated the free-stream static density and velocity could be varied over wide ranges by proper selection of the initial pressures in the various chambers, proportionate lengths of these chambers, and selection of the driver mode. The development of the facility has consisted, in part, of the study of some of these many combinations of options in order to learn what "real-life" limitations might restrict this predicted operational flexibility.

The purpose of this paper is to present the evolutionary process which led to the obtainment of a quasi-steady test flow having an adequate duration for performing aerothermodynamic studies about blunt bodies in the Langley Expansion Tube. Results presented herein were obtained primarily with air and carbon dioxide test gases and with unheated helium as the driver gas. The effects of quiescent test gas pressure, quiescent acceleration gas pressure, type of acceleration gas and secondary diaphragm thickness on test section flow characteristics are discussed. Measured quantities used to evaluate the flow characteristics were time histories of test section pitot pressure and tube wall pressure, along with flow velocity. In the evolutionary process, the obtainment of a quasi-steady flow period of sufficient duration was the first objective. The next objective was to examine the flow quality at this condition. The present study addresses the first objective. Topics such as flow uniformity, test core diameter, run-to-run repeatability, comparison of measured flow quantities to theory and flow establishment about blunt bodies are reported elsewhere.[2,3,5,7]

Description of Expansion Tube

The Langley Expansion Tube[1] is basically a cylindrical tube with a 6-inch (15.24 cm) inside diameter, divided by two (primary and secondary) diaphragms into three sections (see Fig. 1). The upstream section is referred to as the driver or

high-pressure section and is separated from the intermediate or driven section by a square-to-circular double-diaphragm section that can accept either a single diaphragm or two diaphragms. The primary diaphragms are fabricated from stainless steel and have cross-pattern grooves to insure rupture into four triangular petals.[1] As shown in Fig. 1, the intermediate section length can be extended by relocation of the secondary diaphragm. The most downstream section is referred to as the expansion or acceleration section. The acceleration tube is made up of several interchangeable sections to allow changes in the length. A thin Mylar (secondary) diaphragm separates the driven and acceleration sections. Flow through the acceleration section exhausts into a dump tank, and model testing is performed at the exit of the acceleration section; hence, models are tested in an open jet. Schlieren quality windows are located on opposite sides of the dump tank for viewing the flow about test configurations.

A detailed description of the basic components and auxiliary equipment of the Langley Expansion Tube is presented in Ref. 1.

Briefly, the operating sequence for the expansion tube,[6,8,9] which is shown schematically in Fig. 2, begins with the evacuation of all three sections, the test gas and acceleration gas being introduced into the intermediate section and acceleration section, respectively, and the driver section pressurized with the driver gas. Upon rupture of the high-pressure diaphragm, an incident shock wave is propagated into the test gas. The shock wave then encounters and ruptures the low-pressure secondary diaphragm. A secondary incident shock wave propagates into the low-pressure acceleration gas while an upstream expansion wave moves into the test gas. In passing through this upstream expansion wave, which is being washed downstream since the shock-heated test gas is supersonic, the test gas undergoes an isentropic unsteady expansion resulting in an increase in the flow velocity and Mach number.

Survey Rake and Model

Vertical pitot-pressure profiles at the expansion tube test section were obtained with the nine-probe survey rake shown in Fig. 3. This rake has a probe spacing of 0.75 inch (1.905 cm), and the outside diameter of each probe at the sensing surface was 0.31 inch (7.87 mm). The centerline of the center-rake probe was coincident with the expansion tube centerline. Limited results of tests on a sharp-leading-edge flat-plate model, 4 inches (10.16 cm) wide and 9.74 inches (24.74 cm) long, are presented herein. This plate was fabricated from stainless steel and the surface was finished to 16 microinches (0.41 μm).

Instrumentation

Pitot, Wall, and Model Surface Pressure

Pitot pressure, tube wall pressure, and model surface pressure were measured with commercially available miniature piezoelectric (quartz) transducers. These transducers were acceleration-compensated and had rise times of approximately 1 to 3 μs. Each transducer was used in conjunction with a charge amplifier and the output signal was recorded from an oscilloscope with a camera. Thermal protection for the pressure transducer took the form of a circular piece of electrician tape placed over the sensing surface of the transducer. Each pressure transducer and its corresponding charge amplifier was calibrated statically after assembly and positioning in the expansion tube; thus, the transducer, charge amplifier, connecting cables, and oscilloscope were calibrated as a single channel of output. Pitot pressure and tube wall pressure transducers were calibrated periodically during a test series.

Heat-Transfer Rate

Convective heat-transfer rates to the surface of the flat-plate model were obtained using commercially available thin-film resistance

gages having Pyrex 7740 substrates, platinum sensing elements, and silicone monoxide insulating films. Thin-film gages mounted flush with the flat-plate surface survived all tests performed with this model. The maximum percent difference between the initial (factory) calibration and the posttest calibration was 4 percent. Convective heat-transfer rate was determined from the voltage change of the sensing element by means of a computational analysis.[10]

Quiescent Intermediate and Acceleration Section Pressure and Temperature

Quiescent test gas pressure and acceleration gas pressure were measured with high precision, variable capacitance, diaphragm-type differential transducers. The transducers were balanced by exposing both sides of the diaphragm to a low pressure supplied by a cryogenic pump-ion pump combination. This pumping unit supplied the reference pressure during operation. Quiescent acceleration gas temperature was measured with a chromel-alumel thermocouple encased in a stainless-steel shroud. The thermocouple output was read from a compensated digital readout. The quiescent test gas temperature was assumed equal to the measured quiescent acceleration gas temperature.

Velocity

Incident shock velocities in the intermediate section and the acceleration section are routinely measured for each test using a microwave interferometer system[11] and time-of-arrival[12] measurements. The time-of-arrival measurements are also used to infer test gas-acceleration gas interface velocity at the acceleration section exit (test section). A detailed description of these methods used to measure flow velocity is presented in Ref. 12.

Test Conditions

Results presented herein were obtained with an unheated helium driver at a nominal pressure of 5000 psi (34.5 MN/m^2). Because of Joule-Thomson heating and compression heating, the nominal driver temperature exceeded ambient temperature and was 335 K. Air, carbon dioxide, and helium were used as the test gas. Both air and helium were used as the acceleration gas for air test gas, whereas the acceleration gas was the same as the test gas for carbon dioxide and helium. The quiescent test gas pressure for carbon dioxide was varied from 0.5 to 10 psi (3.45 to 68.95 kN/m^2), and the quiescent acceleration gas pressure was varied over a range for all gases. The nominal temperature for the quiescent test gas and acceleration gas was 300 K. The secondary diaphragm was Mylar and thicknesses from 0.00025 to 0.014 inch (6.35 to 355.6 μm) were tested. Intermediate-section and acceleration-section lengths were 15.3 feet (4.66 m) and 55.7 feet (16.98 m), respectively. Pitot pressures presented herein were measured 3 inches (7.62 cm) downstream of the tube exit and on the tube centerline; acceleration section wall pressures were measured 6 feet (1.83 m) upstream of the tube exit, unless specified otherwise.

To provide a means for obtaining accurate test-section conditions, computational schemes for real-air[13] and real-gas mixtures[14] (based on three flow properties measured in the immediate vicinity of the test section) were used. These schemes eliminate an explicit dependence upon measured or calculated upstream flow properties, thereby resulting in a substantial reduction in the uncertainty in predicted test-section flow conditions. The three measured expansion-tube flow parameters serving as input to these schemes for the present study were pitot pressure, free-stream static pressure, and free-stream velocity. The free-stream static pressure was assumed to be equal to the expansion-tube wall pressure measured just upstream of the test section and the free-stream velocity

was assumed to be equal to the acceleration gas-test gas interface velocity, which for the majority of the present conditions was deduced to be equal to the incident shock velocity into the acceleration gas.[3]

Expansion-Tube Flow Characteristics

A number of published[3-5,7] and unpublished aerothermochemistry studies have been performed in the Langley Expansion Tube for various test gases. Contrary to prediction,[6] it was necessary to restrict these studies to a given set of free-stream conditions for each test gas.[3,4] This contradiction between prediction and experiment is believed[3] to be primarily due to boundary layer characteristics along the tube wall, which were not included in prediction.[6] The present paper demonstrates the process used to obtain these free-stream conditions. Time histories of center-line pitot pressure and acceleration section wall pressure were examined over a range of conditions for each test gas and a given helium driver pressure. Variables were quiescent acceleration gas pressure, type of acceleration gas, quiescent test gas pressure, and secondary diaphragm thickness. Variation in these parameters established trends which permitted the best flow conditions to be obtained for each test gas. As defined herein, best flow conditions correspond to the combination of parameters providing maximum quasi-steady test-flow duration. Radial flow uniformity within the test core must also be considered in establishment of best flow conditions. Vertical pitot pressure profiles at the exit of the acceleration section have been presented[2,3] for present test conditions, as have comparisons of measured and predicted shock shapes which verify the existence of uniform flow.[5]

Before presenting measured pitot-pressure time histories, the idealized pitot-pressure time history corresponding to the expansion-tube flow sequence shown in Fig. 2 will be illustrated. A sketch of the ideal

pitot pressure at the acceleration section exit is shown in Fig. 4 as a function of time t. Upon arrival of the incident shock, a sharp increase in pressure occurs. Following a period of constant pressure, a second sharp increase in pressure occurs. This second increase, which is much larger in magnitude than the first, corresponds to the arrival of the acceleration gas-test gas interface. Following the interface arrival, the test-gas pitot pressure is constant over the time interval ψ. This period of constant pressure represents the useful test time, and is terminated by the arrival of the tail of the expansion fan. The primary difference between idealized pitot pressure time histories and measured pitot pressures exhibiting a quasi-steady test-flow duration is the termination of the test flow period. For example, at the end of the test-flow period, the measured pressure may decrease, remain essentially constant but contain large, high-frequency variations in pressure, or increase with time.

Effect of Quiescent Acceleration Gas Pressure

In expansion tube operation, the expansion fan which passes through the shocked test gas lowers the temperature and pressure of the gas and increases the flow velocity. The flow conditions obtained after expansion are dependent on a number of factors, one of the more important being the density (or, for ambient temperature, the pressure) of the quiescent acceleration gas.[6,9] Figure 5 illustrates the effect of quiescent acceleration gas pressure p_{10} on the time history of centerline pitot pressure and acceleration section wall pressure. The quiescent CO_2 test gas pressure was 0.5 psi (3.45 kN/m^2) and the secondary diaphragm was 2.5 x 10^{-4} inch (6.35 μm) thick Mylar. Although not shown in Fig. 5, the centerline pitot pressure $p_{t,c}$ essentially increased linearly with time for values of p_{10} less than 10 μm of Hg (1.33 N/m^2). As p_{10} was increased from the lowest value presented in Fig. 5, $p_{t,c}$ tended to become more

constant with time over a longer time period; however, continued increase in p_{10} ushered in another trend for which the quasi-steady test-flow period Ω diminished with increasing p_{10}. For the range of p_{10} considered, a value of p_{10} around 24 μm of Hg (3.2 N/m^2) appeared to provide the longest value of Ω.

Also shown in Fig. 5 are time histories of the acceleration section wall pressure for various values of p_{10}. The dashed lines denote predicted[15] values of the pressure immediately behind an incident normal shock into CO_2. Ideally, the pressure immediately behind this normal shock remains constant across the acceleration gas-test gas interface and is equal to the tube wall pressure. Measured wall pressures for CO_2 were characterized by a sharp increase upon incident shock arrival followed by a monotonic decrease and then an increase. For the value of p_{10} yielding the "best" pitot pressure time history (p_{10} equal to 24 μm of Hg (3.2 N/m^2)), the maximum measured wall pressure immediately behind the shock and predicted static pressure were in good agreement. However, the difference between measured and predicted pressures increased to approximately 25 percent at a time of 200 μs. This trend of good agreement between prediction and measurement at the time of incident shock arrival was observed for all values of p_{10}. At the three largest values of p_{10}, particularly the largest value, there was evidence of the arrival of the expansion fan. The apparent time of expansion fan arrival, as inferred from the measured wall pressure (see Fig. 5), becomes closer to the time of incident shock arrival as p_{10} increases.

The effect of quiescent pressure on centerline pitot pressure and tube wall pressure time histories is shown in Fig. 6 for air test gas and air acceleration gas. The trends of $p_{t,c}$ with time for air are similar to those for CO_2, with the only significant difference being the

appearance of "spikes" in pressure during the quasi-steady flow period for air. The "best" flow conditions from the viewpoint of pitot pressure time histories occurred for values of p_{10} between approximately 45 to 60 μm of Hg (6 to 8 N/m^2). Wall pressures measured with air test gas also exhibited the same trends with time as wall pressures measured with CO_2. For the range of p_{10} from 45 to 60 μm of Hg (6 to 8 N/m^2), measured wall pressures were within 20 percent of predicted values.[16] The trends of $p_{t,c}$ and p_w with time for helium, nitrogen, and argon test gases were also similar to those for CO_2 and air. (For each test gas, the acceleration gas was the same as the test gas.) Thus, for all test gases examined, a rather limited range of quiescent acceleration gas pressure was observed to yield quasi-steady pitot pressure and wall pressure for a flow duration of approximately 200 to 300 μs. Values of p_{10} outside this small range led to flow conditions unsatisfactory for model testing.

The effect of quiescent acceleration gas pressure on incident shock velocity at the tube exit (test section) and the attenuation of the incident shock velocity along the acceleration section is shown in Fig. 7 for CO_2 test and acceleration gases and Fig. 8 for air test and acceleration gases. For these conditions, the test gas-acceleration gas interface velocity should be essentially equal to the incident shock velocity into the acceleration gas.[3,9] From Figs. 7 and 8, the incident shock velocity is observed to decrease with increasing p_{10}, as expected,[6,8,9,12] and the attenuation in incident shock velocity increases with increasing p_{10}. The incident shock velocity was also observed to decrease with increasing p_{10} for helium, argon, and nitrogen test gases, although the attenuation for the monatomic gases argon and (especially) helium was small.

Calculated[13,14] flow conditions for CO_2 and air test gases are presented in Table 1. The flow for both gases is hypervelocity and hypersonic and appreciable real-gas effects are present. For example, in a hypersonic ideal-air wind tunnel, the maximum possible value of normal shock density ratio ε is 6, whereas, the density ratio for the present air results is approximately 12. The density ratio is used for purposes of illustration since it is the primary factor governing the flow field about blunt bodies at hypersonic speeds. Because helium behaves as an ideal gas at the present expansion tube conditions,[2,3] the range of normal shock density ratio generated in this facility using different test gases is 4 to 19. The upper value of density ratio is nearer to the maximum value expected for Martian or Venusian entry than previously published experimental data, and is believed to be the highest value generated in a ground-based facility for which shock shapes were measured about a stationary model at hypersonic conditions.[3,4,5] In general, the value of p_{10} has a relatively small effect on calculated free-stream and postnormal-shock flow conditions. For example, increasing p_{10} for CO_2 by a factor of 5 decreases the density ratio by only approximately 10 percent and free-stream Mach number by 20 percent.

Effect of Type of Acceleration Gas

In the initial theoretical treatment of expansion tube flow characteristics,[6] it was suggested that the acceleration gas have a small molecular weight. Because of the dangers associated with hydrogen usage, helium was recommended.[6] (Nearly every test performed in the Langley Pilot Model Expansion Tube used helium as the acceleration gas, and this practice was initially carried over to the Langley Expansion Tube.) In Fig. 9, time histories of centerline pitot pressure are shown for air test gas and helium acceleration gas. The data of Figs. 6 and 9 were obtained

under identical conditions and with the same instrumentation, the only difference being the type of acceleration gas employed. The six values of p_{10} for helium in Fig. 9 correspond, theoretically,[9] to the six values of p_{10} for air acceleration gas shown in Fig. 6. (The equivalent p_{10} for helium is approximately 7.2 times that of air.[9]) Comparing the results of Figs. 6 and 9 for equivalent values of acceleration gas pressure, the magnitude of centerline pitot pressure is greater for the helium acceleration gas, implying less of an expansion occurred with helium as with the acceleration gas. The air acceleration gas appears to provide a longer quasi-steady test-flow period and much shorter acceleration gas flow duration, τ. For example, for values of p_{10} equal to 45 and 60 μm of Hg (6 to 8 N/m^2) for air, τ is 25 to 35 μs; however, the corresponding values for p_{10} for helium yeild values of τ between ≈ 100 to 120 μs.

At the lower values of p_{10}, the tube wall pressure for the helium acceleration gas was observed to be greater than the wall pressure for the corresponding value of p_{10} with air. Also, wall pressures for helium acceleration gas were essentially constant with time and did not exhibit the saddlelike characteristic of the wall pressures measured with air acceleration gas. The expected monotonic decrease in velocity with p_{10} was observed for both acceleration gases and with the exception of the highest and lowest values of p_{10} considered, the corresponding velocities between the two acceleration gases were in reasonably good agreement. The attenuation of velocity along the acceleration section was more pronounced for the air acceleration gas than the helium acceleration gas. For air acceleration gas, the velocity attenuation increased with incresing p_{10}, whereas no definite trend was observed for velocity attenuation with helium acceleration gas.

Effect of Quiescent Test Gas Pressure

Since helium driver conditions were approximately constant for the present tests, flow properties behind the incident shock into the test gas were dependent upon the quiescent test gas pressure. As observed previously, the quiescent acceleration gas pressure essentially controlled the extent of the unsteady expansion process. For a given quiescent acceleration gas pressure, a variation in the shock-heated test gas properties in the intermediate section were expected[9] to result in a corresponding variation in expansion-tube test-section flow conditions. In Fig. 10, time histories of centerline pitot pressure measured at the acceleration section exit and acceleration section wall pressure are shown for CO_2 test and acceleration gases for values of quiescent test gas pressure p_1 from 0.5 to 10.0 psi (3.45 to 68.95 kN/m^2) and quiescent acceleration gas pressure equal to 24 μm of Hg (3.2 N/m^2). The quasi-steady test-flow period inferred from $p_{t,c}$ decreased as p_1 was increased from 0.5 to 2.0 psi (3.45 to 13.79 kN/m^2), but the magnitude of pitot pressure and wall pressure were roughly the same. Increasing p_1 to 4 psi (27.58 kN/m^2) yielded results similar to those obtained for 2 psi (13.79 kN/m^2); however, a further increase in p_1 to 10 psi (68.95 kN/m^2) was detrimental to the quality of the pitot pressure with time. Measured and predicted[15] wall pressures were in good agreement and decreased with increasing p_1. Thus, for the range of p_1 examined, the lowest value of 0.5 psi (3.45 kN/m^2) provided the "best" test section flow conditions as inferred from the pitot-pressure time history. For an unheated helium driver pressure of 5000 psi (34.5 MN/m^2), the optimum value of p_1 for all test gases examined thus far was around 0.5 psi (3.45 kN/m^2). The flow velocity for CO_2 was observed to decrease monotonically with increasing p_1 as expected, since the incident shock velocity in the test gas decreased with increasing p_1[12] and the primary factor controlling the expansion process, p_{10} was constant. Flow attenuation along the acceleration section

was nearly constant with p_1. Calculated[14] free stream and postnormal shock flow conditions at the test section are presented in Table 2 for CO_2. The results show the density ratio ε is essentially constant with variation in p_1. Furthermore, variation of free-stream Mach number with p_1 is also small. For the relatively small model size required in expansion tube testing, nonequilibrium flow effects are expected within the shock layer of the model for the present air and CO_2 flow conditions.[5] The free-stream density must be increased significantly[3,5,17] to suppress nonequilibrium effects. However, the results of Table 2 demonstrate this cannot be achieved through increasing p_1 alone.

Effect of Secondary Diaphragm Thickness

In the initial theoretical treatment of the expansion tube,[6] a non-instantaneous rupture of the secondary diaphragm was recognized to be a potential problem to the successful operation of the expansion tube. Even for extremely thin diaphragms, the flow energy lost in the rupture of the diaphragm must result in an upstream-facing shock wave. This shock-reflection is illustrated in Fig. 11, where time histories of the wall pressure 4.25 inches (10.8 cm) upstream of the secondary diaphragm and 3.00 inches (7.62 cm) downstream of the diaphragm are shown for helium, CO_2 and air test gases. The secondary diaphragm is Mylar and is only 2.5×10^{-4} inches (6.35 μm) thick. At the upstream station, which is in the intermediate section, the pressure was essentially constant with time for air and CO_2; however, a sharp increase in the pressure was observed for helium approximately 200 μs after arrival of the incident shock. This pressure increase of approximately 2.8 times the constant pressure for times less than 200 μs is attributed to shock reflection occurring at the secondary diaphragm. Time variation of the wall pressure measured 3.0 inches (7.62 cm) downstream of the diaphragm is similiar for CO_2 and air in that an initial spike was followed by a relatively constant pressure equal to the measured pressure at the upstream location. This

initial sharp increase in pressure (spike) is also attributed to shock reflection at the secondary diaphragm, which was less pronounced than that for helium. That is, the reflected shock for CO_2 and air was quickly weakened and washed downstream. For helium, an initial increase in pressure was also observed at the downstream station, but as plotted, did not appear to be as sharply defined as for CO_2 and air; however, the ratio of the maximum value of the initial pressure increase to the quasi-steady pressure immediately following this increase was roughly 1.5 to 1.65 for all three test gases. The primary difference for helium, as compared to air and CO_2, is that the pressure in the quasi-steady region was significantly greater than the pressure measured at the upstream station for time less than 200 μs. Hence, shock reflection from the secondary diaphragm was more pronounced for helium than for air and CO_2 test gases.

To examine the effect of a noninstantaneous secondary diaphragm rupture on expansion tube flow characteristics, various diaphragm thicknesses were tested. In the present study, Mylar was the only material used for the secondary diaphragm and the thinnest Mylar that could be used on a routine basis with a high degree of reliability in regard to avoiding pinhole leaks was 2.5×10^{-4} inches (6.35 μm) thick. (All data discussed previously were obtained with this thickness, except for $p_1 > 0.5$ psi (3.45 kN/m^2) in Fig. 10 which required thicker diaphragms.)

The effect of secondary diaphragm thickness W on the time history of centerline pitot pressure and acceleration section wall pressure for air test gas ($p_1 = 0.5$ psi (3.45 kN/m^2)) and air acceleration gas ($p_{10} =$ 60 μm of Hg (8 N/m^2)) is shown in Figs. 6(d) and 12. In general, as the diaphragm thickness increased, pitot pressure flow quality diminished, the test flow period decreased, pitot pressure magnitude decreased, then

increased for the thickest diaphragm, measured wall pressure trends remained essentially constant and calculated[16] wall pressures remained constant for values of W to 2 x 10^{-3} inch (50.8 μm), but increased thereafter. From Fig. 13, the measured incident shock velocity at the acceleration section exit was observed to increase with diaphragm thickness, whereas the flow velocity along the acceleration section decreased with distance downstream of the secondary diaphragm for the smaller thicknesses, but increased for thicknesses approximately greater than 2 x 10^{-3} inch (50.8 μm). Thus, a pronounced effect of diaphragm thickness on test section flow conditions exits. For these air data, the measured static pressure immediately behind the incident shock into the quiescent test air was approximately 30 psi (0.207 MN/m^2) at the secondary diaphragm location. This pressure is capable of rupturing 6-inch (15.24 cm) diameter Mylar diaphragms up to a thickness of approximately 3 x 10^{-3} inch (76.2 μm). The calculated[16] pressure behind a corresponding reflected normal shock is approximately 300 psi (2.07 MN/m^2), which is capable of rupturing all diaphragm thicknesses tested.

The secondary diaphragm thickness was also varied for helium test gas (p_1 = 0.5 psi (3.45 kN/m^2)) and helium acceleration gas (p_{10} = 200 μm of Hg (26.66 N/m^2)). Trends of centerline pitot pressure, wall pressure, and incident shock velocity with time were similar to those observed for air as the diaphragm thickness increased, although magnitudes were different. For example, an increase in W from 2.5 x 10^{-4} to 1 x 10^{-2} inch (6.35 to 254 μm) with air resulted in an increase in measured $U_{s,10,e}$ by a factor of 1.15; however, for this same increase in W, measured $U_{s,10,e}$ for helium increased by a factor of approximately 1.35. The measured pressure behind the incident shock into the helium test gas is about 10 psi (68.95 kN/m^2). On a static basis, this pressure is somewhat less than that required to rupture a diaphragm 1 x 10^{-3} inches (25.4 μm) thick. The predicted[18] pressure behind the corresponding reflected shock is only 50 psi (0.345 MN/m^2), as compared to 300 psi (2.07 MN/m^2) for air. For a

given diaphragm material (density), the opening time of the secondary diaphragm is roughly proportional[19] to $\sqrt{W/p_a}$; hence, for a given value of W and assuming that the calculated pressure behind a reflected shock at the secondary diaphragm corresponds to the applied pressure p_a, the secondary diaphragm opening times for helium should be roughly 2.5 times those for air and four times those for CO_2. Conditions yielding the longest opening times should show the most pronounced effects of shock reflection; thus, the effect of shock reflection from the secondary diaphragm is inferred to be more pronounced for helium than for air, as shown previously in Fig. 11.

Flow Establishment About Test Models

As discussed previously, the expansion tube operating sequence differs from other hypersonic-hypervelocity impulse facilities since the model is subjected to the acceleration gas flow prior to the test gas flow. Time histories of shock detachment distance, surface pressure, and surface heat-transfer rate for blunt, axisymmetric models have demonstrated the existence of quasi-steady flow during the latter two-thirds of the approximately 250 μs expansion tube test period for helium, air, and CO_2 test gases.[7] However, no experimental results concerning flow establishment over two-dimensional, relatively long test models in expansion tubes have been published. The time required for the acceleration-gas boundary layer and inviscid flow to relax to the test-gas boundary layer and inviscid flow over a flat plate has been treated theoretically.[20]. A steady-state boundary layer containing more than 95 percent of the test gas ("perfect" nitrogen) was predicted[20] to exist over a plate length equal to three-tenths of the distance traveled by the interface from the leading edge of the flat plate. That is, all the acceleration gas flow in the first foot, or so, over a plate has relaxed to the test gas flow during a 200 μs quasi-steady test period in which the air

interface has traveled approximately 3.5 feet (1.07 m). It should be noted that these predictions[20] are idealized in many respects. To provide some degree of experimental verification, preliminary time histories of surface pressure and heating rate for a sharp-leading-edge flat-plate model are shown in Fig. 14. The test gas was CO_2 and the flow conditions correspond to those presented for CO_2 in Table 1 for p_{10} equal to 24 μm of Hg (3.2 N/m^2). The pressure gage was located 3.6 inches (9.14 cm) downstream of the leading edge and the heat-transfer gage was located 1.05 inches (2.67 cm) from the leading edge. Both measurements indicate a quasi-steady flow was established at these distances downstream of the leading edge within 50 μs, or so, after flow arrival. Also shown in Fig. 14 are photographs of the shock displacement for the sharp-leading-edge flat-plate model in argon flow for various times. Nominal time intervals between successive frames was 10.4 μs. The shock formation was smooth and was observed to be steady approximately 50 to 60 μs after flow arrival. Thus, quasi-steady flow has been obtained about blunt axisymmetric and two-dimensional models during the short test time of expansion tube flow and over a range of flow conditions (test gases).

CONCLUDING REMARKS

The Langley Expansion Tube is an operational facility capable of generating a wide range of real-gas, hypervelocity-hypersonic flow conditions by utilizing a number of different test gases. Measured pitot-pressure and tube-wall pressure time histories were used to define test-section flow quality. For each test gas examined, a rather limited range of quiescent acceleration gas pressure was observed to yield flow quality and test flow durations acceptable for model testing. Optimum test times ranged from 200 to 300 μs and were sufficient to establish flow about blunt axisymmetric test models as well as a sharp-leading-edge flat-plate model. Utilizing helium, air, and CO_2 as the test gas, a range of normal shock

density ratio (primary factor governing the flow field about blunt bodies at hypersonic speeds) from approximately 4 to 19 was calculated. This maximum value of density ratio is believed to be the highest value generated in a ground-based facility for which measurements were obtained about a stationary body at hypersonic conditions. The present results demonstrate that usage of the test gas as the acceleration gas instead of helium, as recommended in NASA TR R-133 and used in all tests performed in the Langley Pilot Model Expansion Tube, provides improved flow quality and longer test times. For the present range of conditions, the optimum quiescent test gas pressure was found to be around 0.5 psi (3.45 kN/m^2). The secondary diaphragm (Mylar) thickness had a pronounced effect on flow quality. This is attributed to the reflected shock from the secondary diaphragm increasing in strength with diaphragm thickness. The thinnest diaphragm yields the best flow conditions; however, a reflected shock was observed for helium test gas even with a secondary diaphragm thickness of only 2.5×10^{-4} inch (6.35 μm).

References

[1]Moore, J. A., "Description and Initial Operating Performance of the Langley 6-Inch Expansion Tube Using Heated Helium Driver Gas," TM X-3240, September 1975, NASA.

[2]Miller, C. G., "Flow Properties in Expansion Tube With Helium, Argon, Air, and CO_2," AIAA Journal, Vol. 12, No. 4, April 1974, pp. 564-566.

[3]Miller, C. G., "Shock Shapes on Blunt Bodies in Hypersonic-Hypervelocity Helium, Air, and CO_2 Flows, and Calibration Results in Langley 6-Inch Expansion Tube," TN D-7800, February 1975, NASA.

[4]Miller, C. G., and Moore, J. A., "Shock Shapes of Blunt Bodies in Hypersonic Helium, Air, and CO_2 Flows," AIAA Journal, Vol. 12, No. 3, March 1974, pp. 411-413.

[5]Miller, C. G., "A Comparison of Measured and Predicted Sphere Shock Shapes in Hypersonic Flows With Density Ratios From 4 to 19," TN D-8076, December 1975, NASA.

[6]Trimpi, R. L., "A Preliminary Theoretical Study of the Expansion Tube, A New Device for Producing High-Enthalpy Short-Duration Hypersonic Gas Flows," TR R-133, 1962, NASA.

[7]Miller, C. G., and Moore, J. A., "Flow-Establishment Times for Blunt Bodies in an Expansion Tube," AIAA Journal, Vol. 13, No. 12, December 1975, pp. 1676-1678.

[8]Miller, C. G., "A Program for Calculating Expansion-Tube Flow Quantities for Real-Gas Mixtures and Comparison With Experimental Results," TN D-6830, September 1972, NASA.

[9]Miller, C. G., and Wilder, S. E., "Program and Charts for Determining Shock Tube, Expansion Tube, and Expansion Tunnel Flow Quantities for Real Air," TN D-7752, February 1975, NASA.

[10]Cook, W. J., and Felderman, E. J., "Reduction of Data From Thin-Film Heat-Transfer Gages: A Concise Numerical Technique,: AIAA Journal, Vol. 4, No. 3, March 1966, pp. 561-562.

[11]Laney, C. C., "Microwave Interferometry Technique for Obtaining Gas Interface Velocity Measurements in an Expansion Tube Facility," TM X-72625, November 1974, NASA.

[12]Miller, C. G., and Jones, J. J., "Incident Shock-Wave Characteristics in Air, Argon, Carbon Dioxide, and Helium in a Shock Tube With Unheated Helium Driver," TN D-8099, December 1975, NASA.

[13]Miller, C. G., and Wilder, S. E., "Real-Air Data-Reduction Procedures Based on Flow Parameters Measured in the Test Section of Supersonic and Hypersonic Facilities," TN D-6618, March 1973, NASA.

[14]Miller, C. G., "Computer Program of Data Reduction Procedures for Facilities Using CO_2-N_2-O_2-Ar Equilibrium Real-Gas Mixtures," TM X-2512, March 1972, NASA.

[15]Miller, C. G., and Wilder, S. E., "Tables and Charts of Equilibrium Normal Shock and Shock Tube Properties For Pure Carbon Dioxide With Velocities From 1 to 16 km/sec.," SP-3100, 1977, NASA.

[16]Feldman, S., "Hypersonic Gas Dynamic Charts for Equilibrium Air," Res. Rep. 40, January 1957, Avco-Everett Res. Lab.

[17]Olstad, W. B., Jones, J. J., Sutton, K., and Walberg, G. D., "Langley Research Center Entry Aerothermodynamic Technology Development in Support of Pioneer Venus Multiprobe Mission Studies," AIAA Conference on the Exploration of the Outer Planets,St. Louis, Missouri, September 1975, AIAA Paper No. 75-1161.

[18]Gaydon, A. G., and Hurle, I. R., "The Shock Tube in High-Temperature Chemical Physics,"Reinheld Pub. Corp., 1963.

[19]Simpson, C. J. S. M., Chandler, T. R. D., and Bridgman, K. G., "Effect on Shock Trajectory of the Opening Time of Diaphragms in a Shock Tube," Phys. Fluids, Vol. 10, No. 9, September 1967, pp. 1894-1896.

[20]Gupta, R. N., "An Analysis of the Relaxation of Laminar Boundary Layer on a Flat Plate After Passage of an Interface With Application to Expansion-Tube Flow," TR R-397, December 1972, NASA.

TABLE 1. CALCULATED FREE STREAM AND POSTNORMAL SHOCK FLOW CONDITIONS FOR EQUILIBRIUM AIR AND CO_2 TEST GASES OVER A RANGE OF QUIESCENT ACCELERATION GAS PRESSURE

p_{10}, μm of Hg	p_{10}, (N/m^2)	p_∞, N/m^2	T_∞, K	$\gamma_{E,\infty}$	U_∞, m/s	M_∞	$N_{Re,\infty}$, $m^{-1} \times 10^{-5}$	ε	$\gamma_{E,s}$	p_{sp}, $N/m^2 \times 10^{-5}$	T_{sp}, K
Air											
15	(2)	689	1277	1.317	5859	8.43	2.27	12.69	1.134	0.63	6258
30	(4)	1138	977	1.338	5612	9.16	5.49	12.00	1.140	1.24	6274
45	(6)	1931	1327	1.314	5401	7.63	5.51	11.37	1.143	1.43	6227
60	(8)	2344	1326	1.314	5307	7.50	6.58	11.12	1.145	1.68	6205
90	(12)	3861	1821	1.282	5108	6.24	6.18	10.45	1.147	1.88	6176
180	(24)	5309	2149	1.239	4729	5.40	5.94	9.52	1.154	1.88	5957
CO_2											
14	(1.9)	758	1367	1.167	5197	9.46	3.18	19.09	1.164	0.78	3934
24	(3.2)	1151	1157	1.176	4954	9.77	6.06	19.03	1.149	1.27	3820
37	(4.9)	1586	1329	1.169	4793	8.84	6.44	18.51	1.145	1.43	3771
50	(6.7)	2344	1534	1.157	4672	8.06	7.29	17.86	1.143	1.74	3772
67	(8.9)	2965	1672	1.143	4597	7.64	7.84	17.41	1.143	1.95	3775

TABLE 2. CALCULATED FREE STREAM AND POSTNORMAL SHOCK FLOW CONDITIONS FOR EQUILIBRIUM CO_2 TEST GAS OVER A RANGE OF QUIESCENT TEST GAS PRESSURE

p_1, psi	p_1, (kN/m^2)	p_∞, N/m^2	T_∞, K	$\gamma_{E,\infty}$	U_∞, m/s	M_∞	$N_{Re,\infty}$, $m^{-1} \times 10^{-5}$	ε	$\gamma_{E,s}$	p_{sp}, $N/m^2 \times 10^{-5}$	T_{sp}, K
0.5	(3.45)	1151	1157	1.176	4954	9.77	6.06	19.03	1.149	1.27	3820
2.0	(13.79)	1103	1113	1.177	4640	9.33	5.80	18.87	1.136	1.11	3605
4.0	(27.58)	931	724	1.200	4454	10.99	9.64	19.10	1.128	1.32	3483
10.0	(68.95)	793	507	1.228	4054	11.83	14.20	18.53	1.117	1.34	3257

ORIGINAL PAGE IS
OF POOR QUALITY

Page
Intentionally
Left Blank

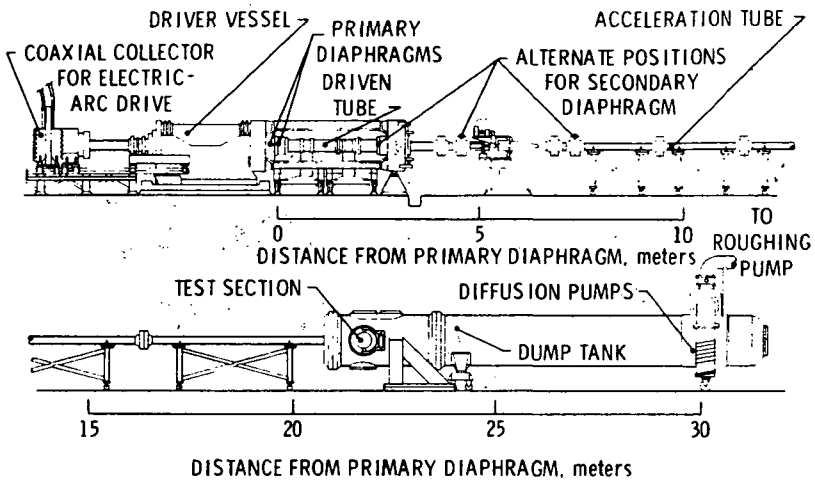

Figure 1. Sketch of Langley Expansion Tube.

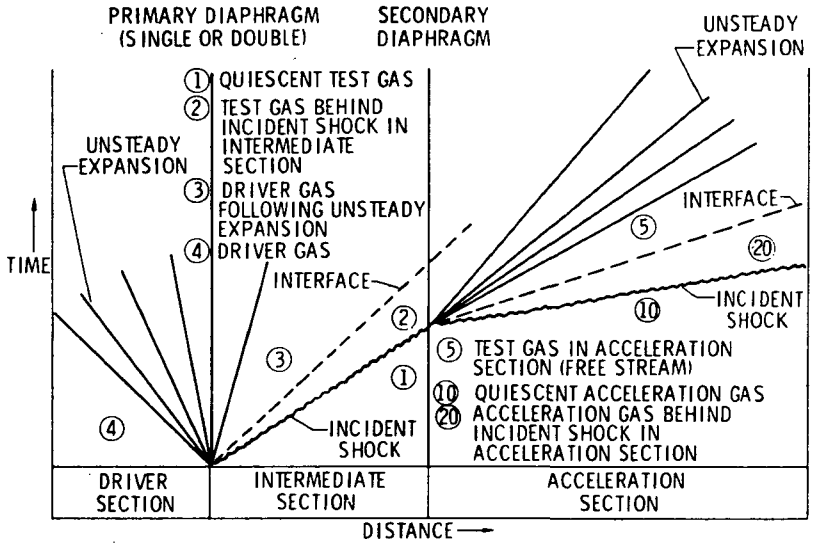

Figure 2. Schematic diagram of expansion-tube flow sequence.

ORIGINAL PAGE IS
OF POOR QUALITY

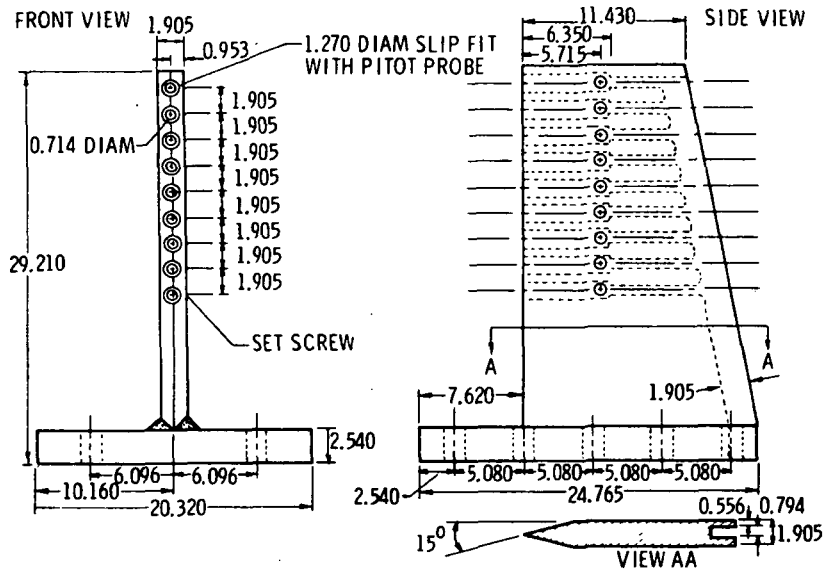

(a) Pitot-pressure survey rake probe holder.

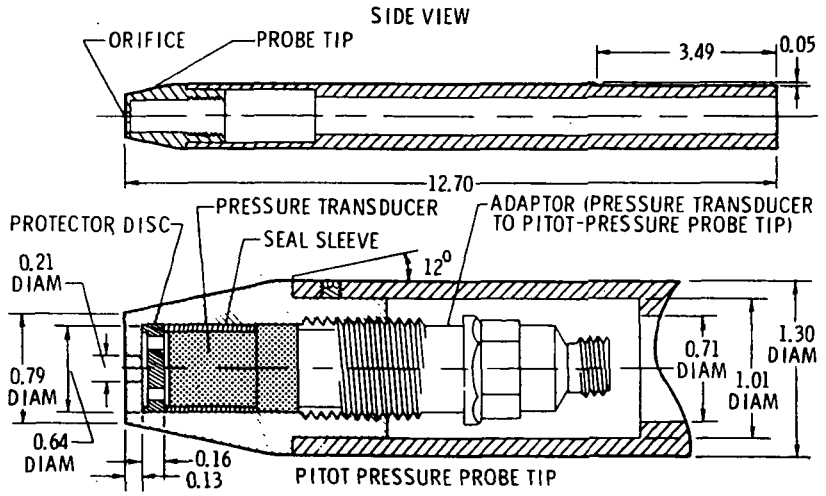

(b) Pitot-pressure probe.

Figure 3. Pitot-pressure survey rake and probe.
All dimensions in centimeters.

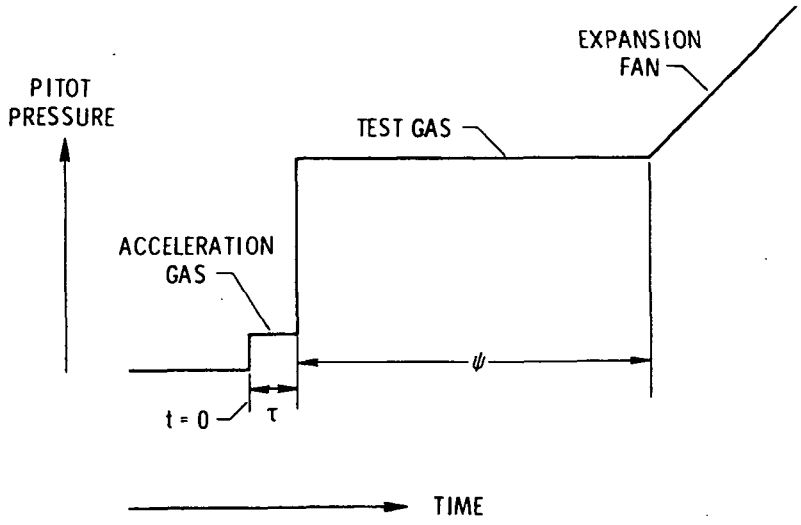

Figure 4. Sketch of idealized pitot pressure time history at exit of acceleration section.

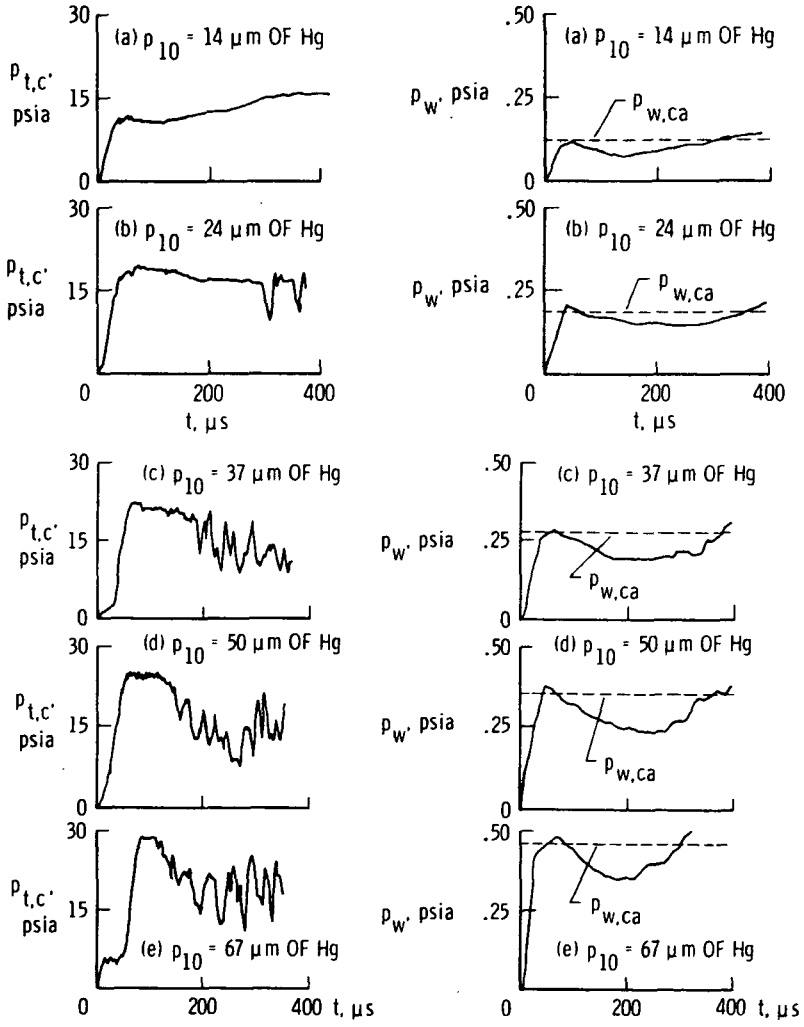

Figure 5. Effect of quiescent acceleration gas pressure on time history of centerline pitot pressure and tube wall pressure for CO_2 test gas and CO_2 acceleration gas.

ORIGINAL PAGE IS
OF POOR QUALITY

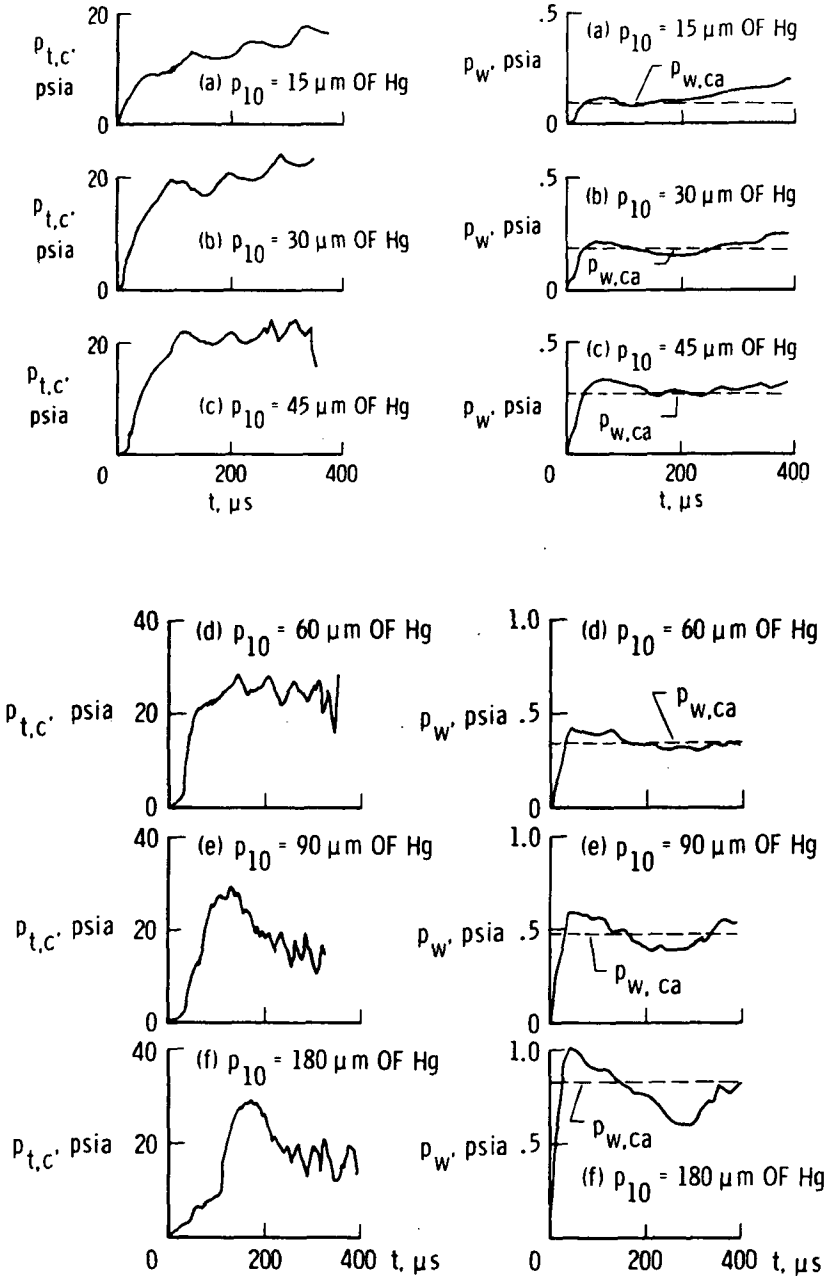

Figure 6. Effect of quiescent acceleration gas pressure on time history of centerline pitot pressure and tube wall pressure for air test gas and air acceleration gas.

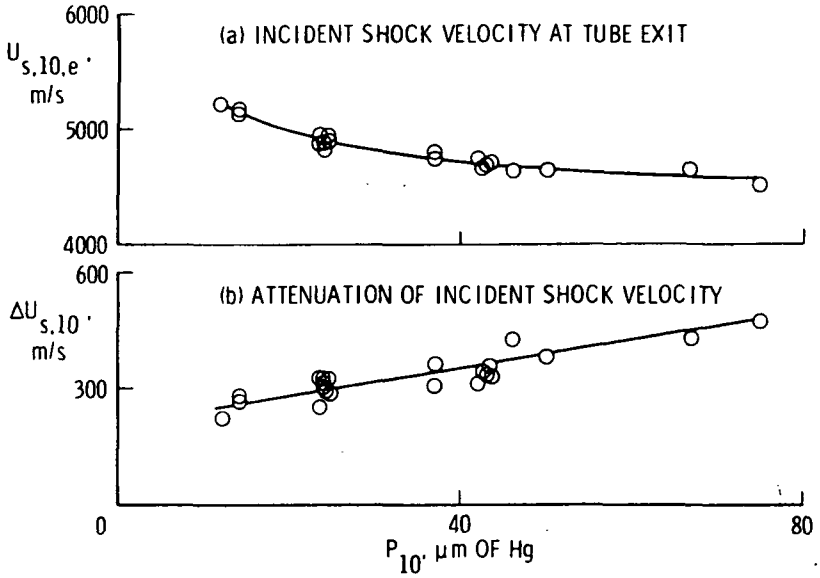

Figure 7. Effect of quiescent acceleration gas pressure on incident shock velocity at tube exit and attenuation of incident shock velocity along acceleration section for CO_2 test gas and CO_2 acceleration gas.

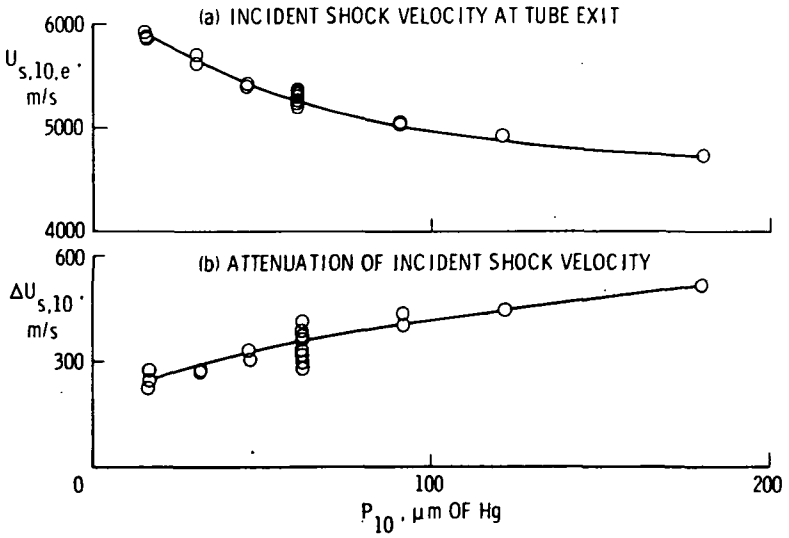

Figure 8. Effect of quiescent acceleration gas pressure on incident shock velocity at tube exit and attenuation of incident shock velocity along acceleration section for air test gas and air acceleration gas.

ORIGINAL PAGE IS
OF POOR QUALITY

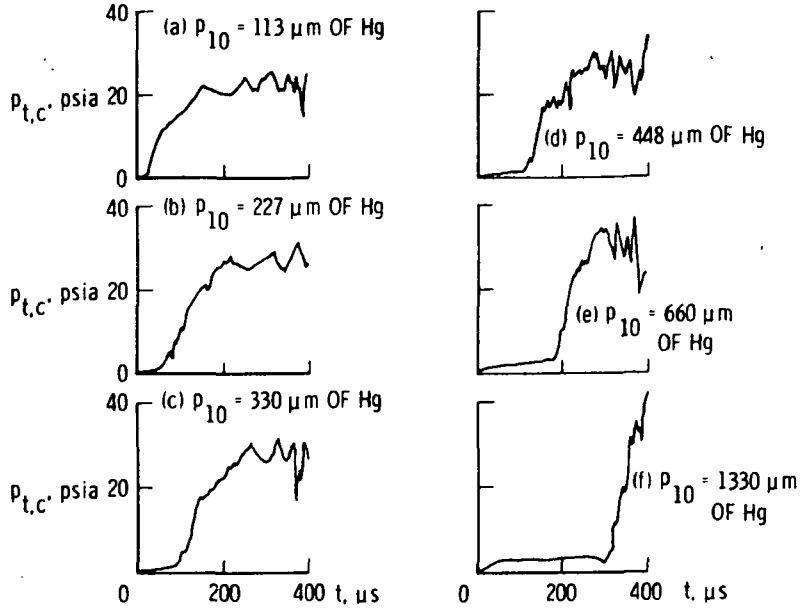

Figure 9. Effect of quiescent acceleration gas pressure on time history of centerline pitot pressure for air test gas and helium acceleration gas.

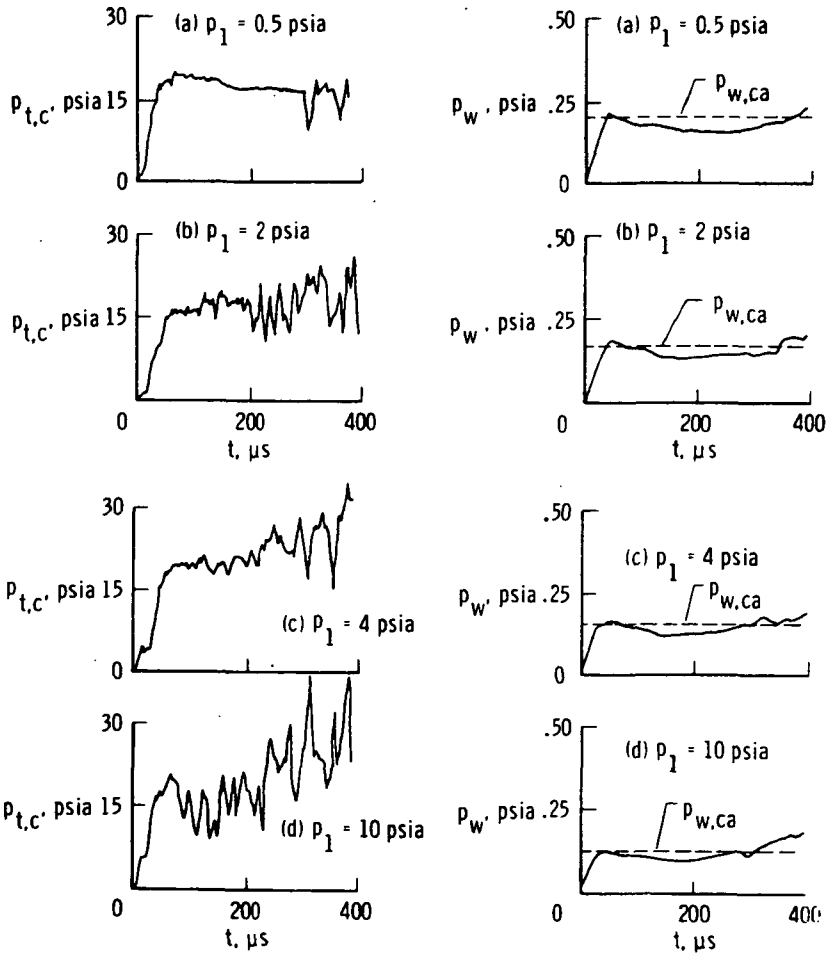

Figure 10. Effect of quiescent test gas pressure on time history of centerline pitot pressure and tube wall pressure for CO_2 test gas and CO_2 acceleration gas.

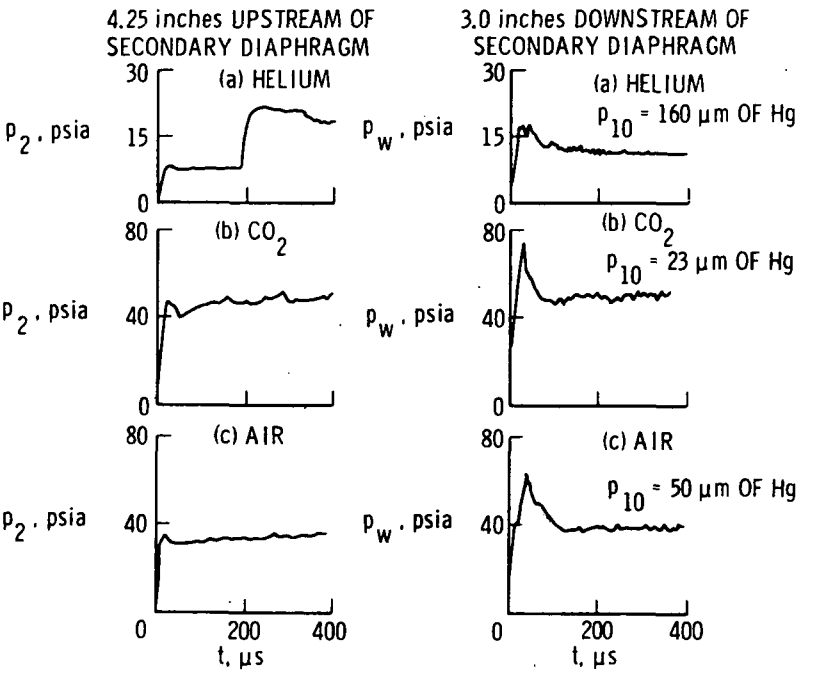

Figure 11. Time history of tube wall pressure immediately upstream and immediately downstream of the secondary diaphragm for helium, CO_2, and air test gases. p_1 = 0.5 psi (3.45 kN/m^2).

ORIGINAL PAGE IS
OF POOR QUALITY

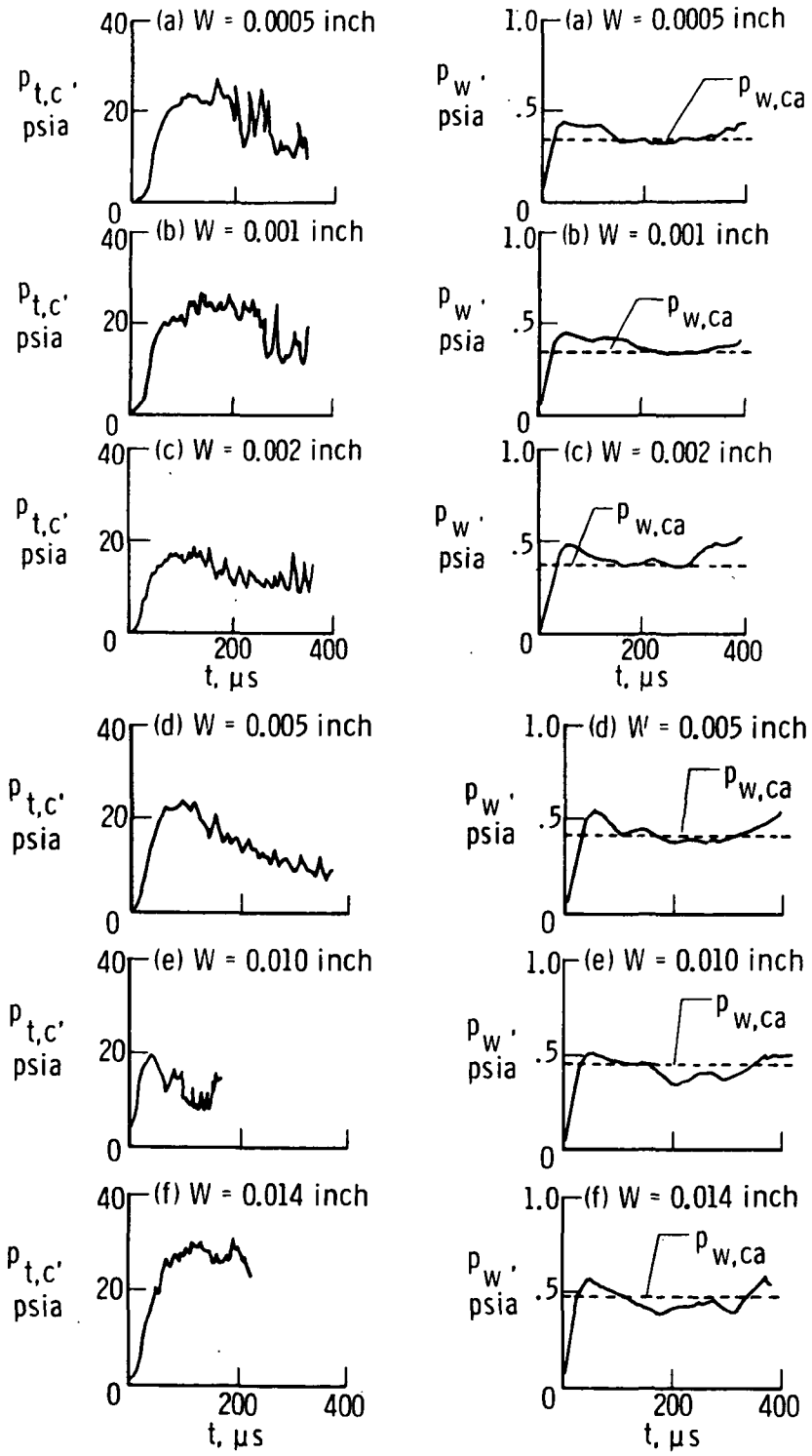

Figure 12. Effect of secondary diaphragm thickness on time history of centerline pitot pressure and tube wall pressure for air test gas and air acceleration gas.

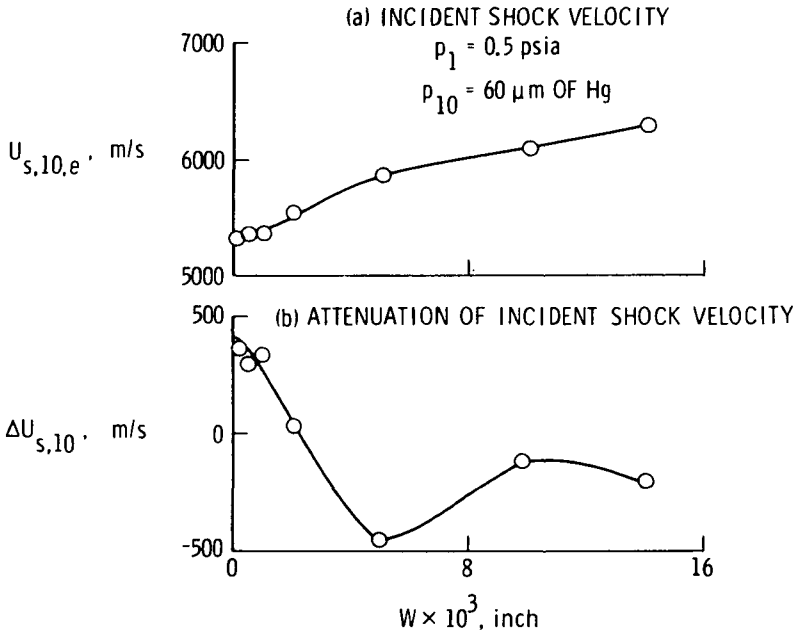

Figure 13. Effect of secondary diaphragm thickness on incident shock velocity at the tube exit and attenuation of incident shock velocity along acceleration section for air test gas and air acceleration gas.

ORIGINAL PAGE IS
OF POOR QUALITY

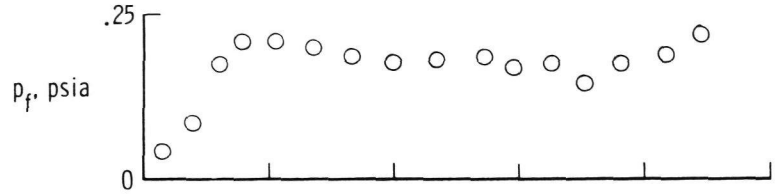

(a) Flat-plate surface pressure; CO_2 test gas.

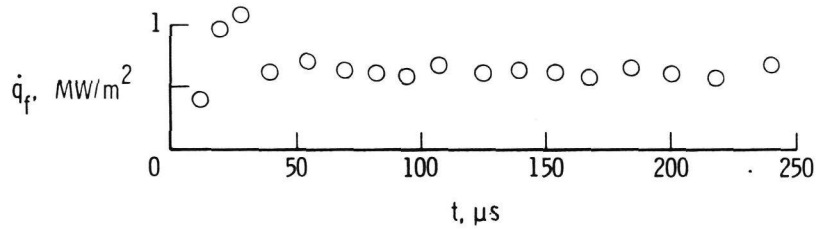

(b) Flat-plate surface heating rate; CO_2 test gas.

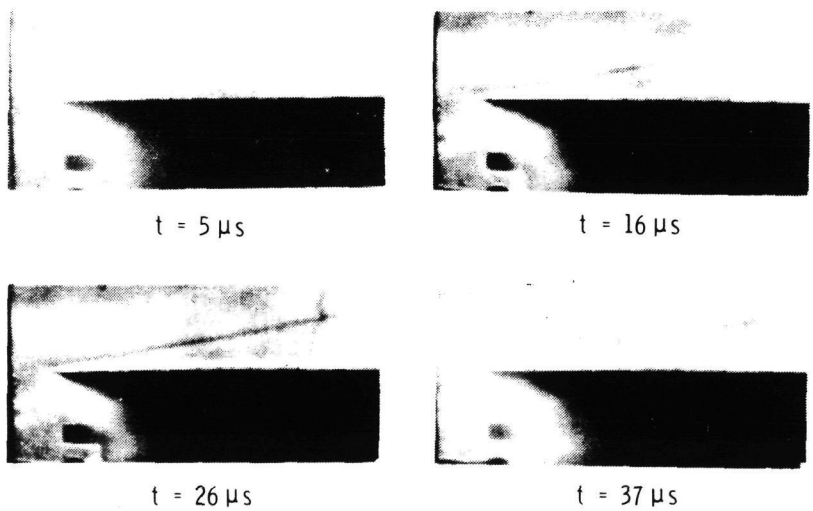

(c) Shock shape establishment; argon test gas.

Figure 14. Time histories of surface pressure and heating rate and shock shape establishment for sharp-leading-edge flat-plate model.